https://doi.org/10.5194/egusphere-2026-5769
Preprint. Discussion started: 2 October 2026
© Author(s) 2026. CC BY 4.0 License.

# Greenland fjord processes have a depth-dependent influence on predicted submarine melt rates

Emma F. Cameron[1, 2], Tom R. Cowton[1], Alexander T. Bradley[3], and Paul R. Holland[2]

[1]School of Geography and Sustainable Development, University of St Andrews, St Andrews, UK
[2]British Antarctic Survey, Cambridge, UK
[3]Department of Geography, King's College London, London, UK

**Correspondence:** Emma F. Cameron (efc4@st-andrews.ac.uk)

**Abstract.** Recent ice loss from the Greenland Ice Sheet has been driven in part by the retreat of marine-terminating glaciers in response to ocean warming. Efforts to quantify ocean forcing often rely on far-field ocean properties, which differ from those adjacent to glacier termini in fjords. To quantify these differences and their significance for glacier ablation, we analyse 58 pairs of near-glacier and fjord-mouth conductivity-temperature-depth measurements from 38 fjords around Greenland collected between 2016 and 2021. Relative to fjord mouth properties, near-glacier profiles show consistent near-surface cooling, attributed to iceberg melt, and intermediate-depth warming caused by plume-driven upwelling of deeper waters. Available results from Southeast Greenland appear different, with near-glacier waters colder and fresher than fjord mouths at all depths. Our results show that while it is generally reasonable to use shelf water properties to model submarine melt at depths > 250 m (except for fjords with shallow sills), this approach will significantly overestimate melt near the surface and underestimate at mid depth, potentially influencing the predicted rate of glacier ablation.

## 1 Introduction

The Greenland Ice Sheet has lost significant mass over the past few decades, in part due to changes in ice dynamics driven by calving and submarine melting at marine-terminating glaciers (Otosaka et al., 2023; Mankoff et al., 2021; Wood et al., 2021; Holland et al., 2008). This submarine melting acts as both a direct source of mass loss and a driver of glacier calving Motyka et al. (2003); Slater et al. (2021). In recent decades, periods of warmer waters on the continental shelf in Southeast Greenland and Disko Bay have been associated with periods of glacier retreat, acceleration and thinning (Howat et al., 2008; Bevan et al., 2019; Holland et al., 2008; Motyka et al., 2011).

Submarine melt rates depend on the temperature, salinity and velocity of adjacent fjord waters Jenkins (2011). Many of Greenland's fjords are connected to dense and warm Atlantic-origin waters (AW) at the continental slope by deep cross-shelf troughs. Although the hydrography of the East and West Greenland continental shelves differ, both regions share a similar structure: Atlantic Water (AW) reaches fjord mouths through these deep cross-shelf troughs, while colder, fresher Arctic-origin

https://doi.org/10.5194/egusphere-2026-5769
Preprint. Discussion started: 2 October 2026
© Author(s) 2026. CC BY 4.0 License.

water overlies it across most of the shallow shelf (Sutherland and Pickart, 2008; Rysgaard et al., 2020, 2024; Mortensen et al., 2022).

As shelf waters transit fjords they can be substantially modified by a range of interacting physical processes (Straneo and Cenedese, 2015). Subglacial-discharge plumes released at glacier grounding lines drive overturning circulation, whereby buoyant turbulent plumes entrain and transport deep waters to shallower depths, redistributing heat throughout the water column (Jenkins, 2011; Straneo and Cenedese, 2015). Where grounding lines are in contact with AW, this vigorous upwelling can drive substantial local submarine melting while also enhancing ambient melt across the ice front (Slater et al., 2018). Iceberg melting further cools and freshens fjord waters and can modify fjord circulation through buoyancy-driven upwelling (Davison et al., 2020, 2022; Mortensen et al., 2020). Exchange with the continental shelf is additionally influenced by wind-driven forcing, coastal trapped waves, and storm events, which can episodically renew fjord waters and alter their hydrographic structure (Jackson et al., 2014; Fraser et al., 2018; Spall et al., 2017). Within fjords, tidal mixing promotes vertical exchange (Geyer and Cannon, 1982; Mortensen et al., 2011), while shallow sills can inhibit the inflow of deep AW, leading to cooler and fresher fjord waters than those on the adjacent shelf (Gladish et al., 2015; Mortensen et al., 2011; Bao and Moffat, 2024; Nilsson et al., 2023). Sills can also promote the recirculation (or reflux) of glacially modified waters, further amplifying fjord cooling and freshening (Hager et al., 2022). Collectively, these processes can substantially alter the hydrographic properties of waters entering fjords before they interact with glacier termini, highlighting the need for methods that infer fjord water properties from shelf observations while accounting for fjord-scale modification processes.

In order to better understand the role of ocean forcing in the retreat of Greenland's glaciers, we need to understand how fjords modify the temperatures of waters reaching fjord interiors at a Greenland-wide scale. Fjords are generally too small to be resolved by large-scale ocean, ice, and climate models (Smith et al., 2021; Goelzer et al., 2020; Watanabe et al., 2010, for example). To address this, submarine melting is commonly parameterised using formulations that relate melt rates to subglacial discharge and thermal forcing (Rignot et al., 2016), which is often derived from offshore ocean conditions and simplified representations of fjord geometry (Slater et al., 2020). While these approaches aim to approximate conditions at glacier grounding lines, it remains uncertain how well offshore water properties represent fjord and ice–ocean boundary conditions at Greenland-wide scales.

Cowton et al. (2023) studied fjord water properties at 14 glaciers in North West Greenland and found characteristic warming at intermediate depths inside fjords relative to shelf water properties, associated with the upwelling of deep AW by subglacial discharge plumes. Here we expand on this study to include 38 fjords from across Greenland to assess whether these findings are reproducible for fjords at a Greenland-wide scale, using CTD profiles from the Oceans Melting Greenland (OMG) project (Fenty et al., 2016; OMG, 2019, 2020). We compare synoptic CTD profiles at the mouth and head of each fjord (taken within 72 hous of each other) to investigate (i) how fjord processes modify the temperature profile of water adjacent to the glacier relative to the fjord mouth, (ii) the physical mechanisms driving these changes at a Greenland-wide scale, and (iii) the implications for predictions of submarine melt rates that assume thermal forcing near the glacier matches that offshore.

https://doi.org/10.5194/egusphere-2026-5769
Preprint. Discussion started: 2 October 2026
© Author(s) 2026. CC BY 4.0 License.

## 2 Methods

### 2.1 Sampling near-glacier and fjord-mouth pairs

Fig. 1 shows the location of temperature and salinity profiles from ship-borne CTDs and airborne expendable CTD instruments (AXCTDs) from the OMG project (Fenty et al., 2016; OMG, 2019, 2020). Hereafter, AXCTDs and CTDs are collectively referred to as CTDs. These surveys were taken in August to October between 2015 and 2021. At this time of year subglacial discharge is receding from its July peak (King et al., 2018) and sea ice is at its annual minimum (Meier and Stroeve, 2022).

Fjords included in the full OMG dataset were retained in our study if the fjord met the following criteria: (1) the fjord has a marine terminating glacier at its head; (2) the fjord contains a CTD collected within 10 km of the glacier terminus and inshore of the shallowest sill; (3) the dataset contains a second CTD collected within 20 km of the fjord mouth, representing water entering the fjord from the continental shelf; and (4) the two CTDs were collected within 3 days of each other to reduce the effects of synoptic-scale variability (Jackson et al., 2014). Exceptions to this are at Kangerlussuaq Fjord (Kangersertuaq) and Sermilik fjord where dense mélange means that near-glacier CTDs were obtained 20km from the terminus.

For each fjord, a CTD at the fjord mouth was selected as indicative of the properties of shelf waters entering the fjord. We chose to sample within the fjord mouth, rather than outside the fjord, because strong cross-shelf temperature and salinity gradients can cause water properties to change quickly with distance from the fjord, particularly in southeast Greenland, where the East Greenland Coastal Current/East Greenland Current and Irminger Current converge near the continental slope (Sutherland and Pickart, 2008). Furthermore, shelf currents may be topographically steered in ways that limit ingress of water to fjords (Sutherland et al., 2014). By sampling within the fjord mouth, we can be confident that the observed water properties are representative of shelf waters entering fjords, better allowing us to isolate the impacts of water modification that takes place within the fjords themselves.

Fjords are grouped by region into Northwest (NW), Central West (CW), Central East (CE) and Southeast (SE) Greenland. We do not include South West, North and North East Greenland as they have fewer CTDs available from the Oceans Melting Greenland project, which we used to limit the practical scope of the study.

In this study, sill and grounding line depths are from Mas e Braga (2025) where available, but otherwise are computed using BedMachine v5 bathymetry data (Morlighem et al., 2022). To measure the distance between the near-glacier CTD and the glacier termini the terminus position was digitised from the nearest satellite passover using the Google Earth Engine Digitisation Tool v2.04 (Lea, 2018). Each fjord is given a unique identifying number, based on the numbering system of glaciers in Goliber et al. (2021), combined with the year of acquisition.

### 2.2 Data processing

Temperature and salinity from each near-glacier and fjord-mouth CTD pair were converted to conservative temperature and absolute salinity using the GSW Oceanographic Toolbox (TEOS-10) (McDougall and Barker, 2011), averaged into 10 m vertical bins, and the depth-dependent differences calculated as:

https://doi.org/10.5194/egusphere-2026-5769
Preprint. Discussion started: 2 October 2026
© Author(s) 2026. CC BY 4.0 License.

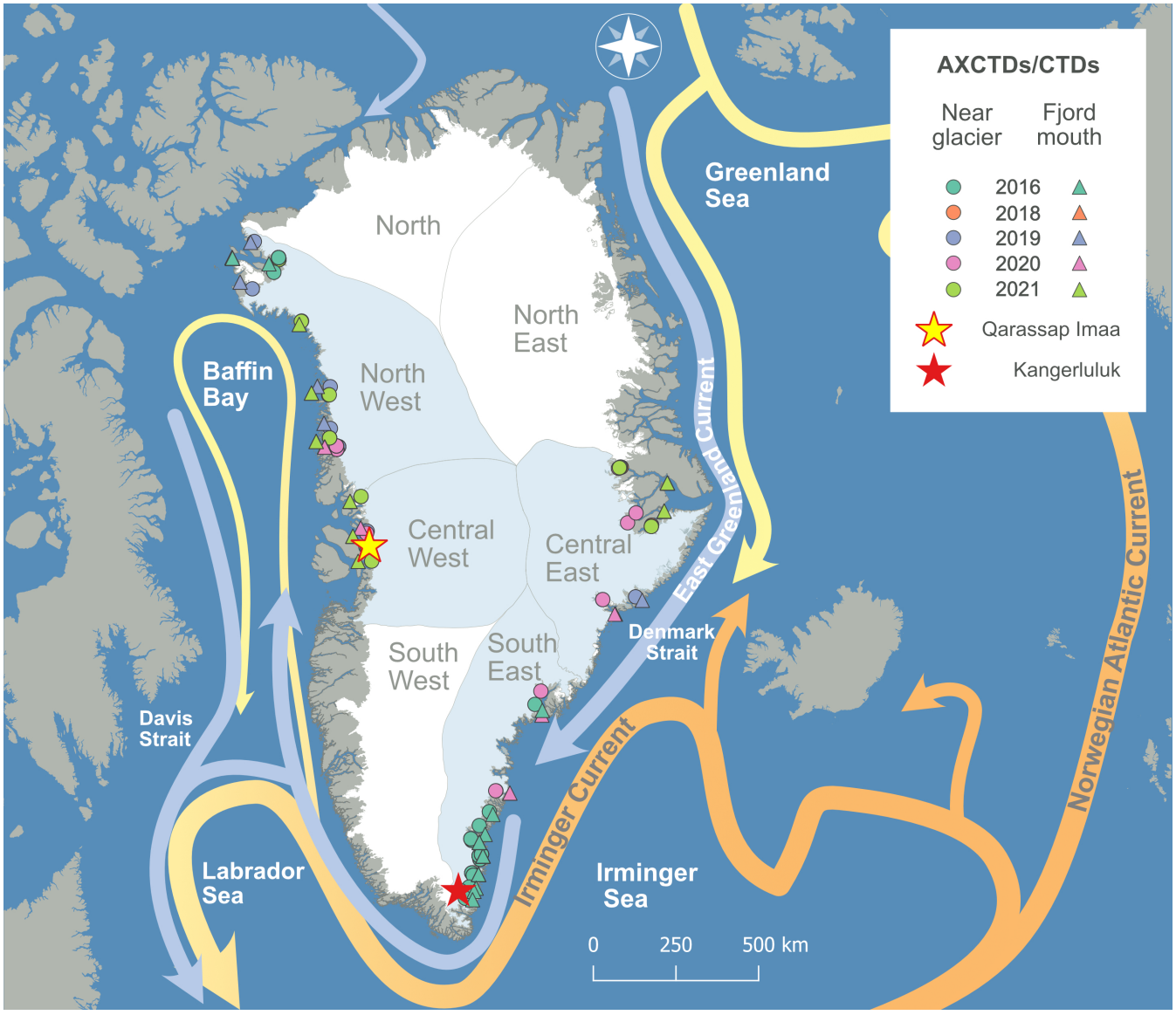


**Figure 1.** Map of Greenland, showing CTD locations used in this study. Starred locations are the fjords used as case studies in Section 3.3. Study regions are shaded in blue, with region outlines taken from Mouginot et al. (2019). Arrows represent major currents around the Greenland Ice Sheet based on Straneo et al. (2012). Currents transporting warm, Atlantic-origin waters are in orange and yellow, while currents transporting cold and fresh Arctic-origin waters are in blue.

$$\delta\Theta(z) = \Theta_{\text{glacier}}(z) - \Theta_{\text{mouth}}(z), \tag{1}$$

and

https://doi.org/10.5194/egusphere-2026-5769
Preprint. Discussion started: 2 October 2026
© Author(s) 2026. CC BY 4.0 License.

$$\delta S(z) = S_{\text{glacier}}(z) - S_{\text{mouth}}(z), \tag{2}$$

where $z$ is depth; $\Theta_{\text{glacier}}$ and $S_{\text{glacier}}$ are the near-glacier conservative temperature and absolute salinity, and $\Theta_{\text{mouth}}$ and $S_{\text{mouth}}$ are the mouth values. Positive $\delta\Theta$ indicates the near-glacier profile is warmer than the mouth, and positive $\delta S$ indicates it is more saline.

The depth-dependent percentage difference in melt rate (PDS) is adapted from Jackson et al. (2014) as:

$$PDS(z) = \frac{\dot{m}_{\text{glacier}}(z) - \dot{m}_{\text{mouth}}(z)}{\dot{m}_{\text{mouth}}(z)} \times 100 = \frac{TF^{\beta}_{\text{glacier}}(z) - TF^{\beta}_{\text{mouth}}(z)}{TF^{\beta}_{\text{mouth}}(z)} \times 100, \tag{3}$$

where $\dot{m}_{\text{glacier}}$ and $\dot{m}_{\text{mouth}}$ are the submarine melt rates associated with the near-glacier CTD profile and mouth CTD profile respectively. $TF$ is thermal forcing (i.e. the conservative temperature minus the conservative temperature freezing point of seawater at that depth), and $\beta$ is an exponent that determines the sensitivity of the melt rate to thermal forcing (Xu et al., 2013; Rignot et al., 2016; Slater et al., 2020). The exponent $\beta$ ranges from 1.6 in fjords with low subglacial discharge to 1.2 in fjords with high subglacial discharge rates (Xu et al., 2013). Here we assign a value of 1.2, as subglacial discharge remains significant in late summer, but note that this may lead to an underestimation of the sensitivity of melt rates to fjord water modification. Results obtained using a scaling $\beta = 1.6$ can be found in Appendix A, Fig. A1. Each profile was first binned onto a global 10 m grid from 0-1000 m, and empty values were masked. PDS profiles were only calculated down to grounding line depth (or the depth of the shallower profile) as water below grounding line depth is not in contact with ice.

## 3 Results

### 3.1 Along-fjord temperature changes

We find consistent regional-scale patterns of fjord temperature modification with depth (Fig. 2). Surface waters near glaciers are typically 4 to 6°C cooler than at the fjord mouth, while waters at intermediate depths ($\sim$ 50 to 250 m) can be 1 to 2°C warmer. The salinity difference between the fjord mouth and near-glacier environment is highly variable at the surface, and becomes less variable with depth, except in SE Greenland (Fig. 2e-h). Cold and fresh anomalies at depth are likely associated with shallow sills that obstruct AW inflow into the fjord (Bao and Moffat, 2024; Hager et al., 2022).

Results from SE Greenland appear different, with the entire water column typically appearing as colder and fresher near glaciers relative to fjord mouths, albeit with high inter-fjord variability and (Figures 2d,h). Kangersertuaq Fjord (a large fjord adjacent to Kangerlussuaq glacier in CE Greenland) also shows a pronounced deep cold anomaly (Fig. 2c, Fig. A2). Analysis of these patterns is presented in Section 3.3.

https://doi.org/10.5194/egusphere-2026-5769
Preprint. Discussion started: 2 October 2026
© Author(s) 2026. CC BY 4.0 License.

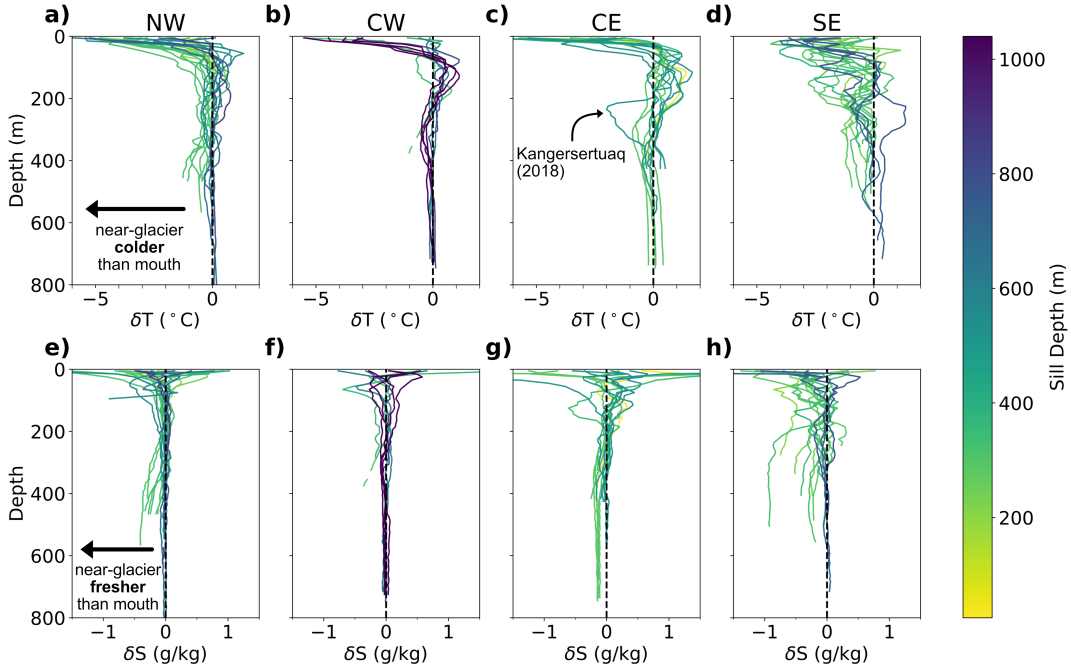


**Figure 2.** Temperature and salinity difference plots, coloured by sill depth (as indicated in the colourbar) for: North West (NW) Greenland (a, e); Central West Greenland (CW) (b, f); Central East Greenland (CE) (c, g); Southeast Greenland (SE) (d, h). Positive temperature anomalies ($\delta T > 0$) represent depths where the water in the near-glacier profile is warmer. Negative salinity anomalies ($\delta S < 0$) occur where near-glacier water properties are fresher than the mouth profile.

### 3.2 The effect on submarine melt rates

Thermal forcing is commonly used to represent the ocean heat available to drive submarine melting, and is a key term in glacier ablation parameterisations used by large ice sheet models (Slater et al., 2020). However, Fig. 2 shows that water temperatures change towards the glacier, meaning that the thermal forcing experienced at the glacier terminus may differ from that measured at the fjord mouth. To quantify this difference, we calculated the depth-dependent difference in thermal forcing ($\delta TF$) between the near-glacier region and the fjord mouth at each depth for each CTD pair:

$$\delta TF(z) = TF_{\text{glacier}}(z) - TF_{\text{mouth}}(z). \tag{4}$$

Positive $\delta TF$ values indicate greater thermal forcing near the glacier than at the fjord mouth at the given depth, whereas negative values indicate reduced thermal forcing near the glacier. To understand how this pattern changes at different depths, $\delta TF$ was binned into three depth ranges: shallow (0–<50 m), intermediate (50–<250 m), and deep (≥250 m). Each CTD pair contributed one mean $\delta TF$ value to each depth range (Fig. 3).

https://doi.org/10.5194/egusphere-2026-5769
Preprint. Discussion started: 2 October 2026
© Author(s) 2026. CC BY 4.0 License.

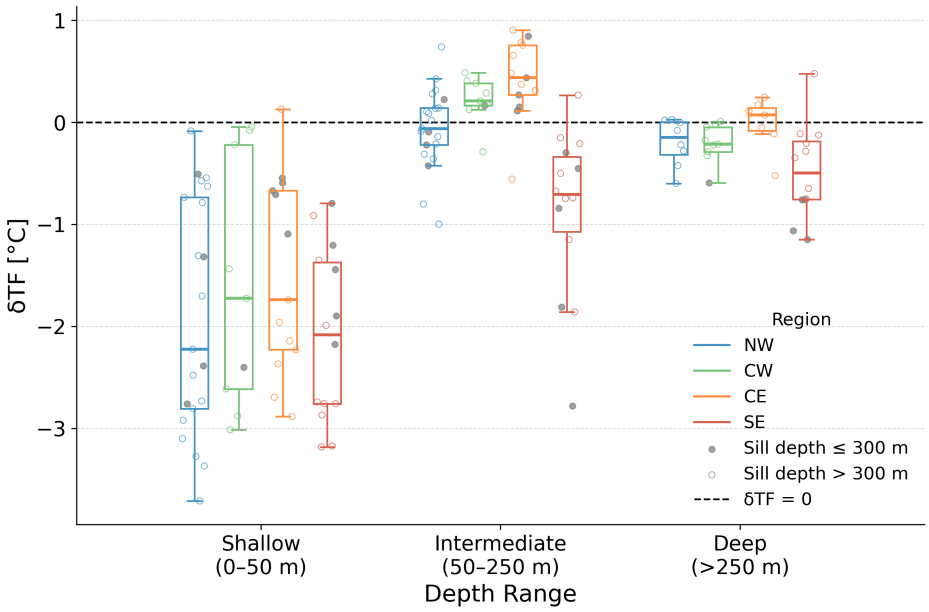


**Figure 3.** Boxplots showing the difference in thermal forcing ($\delta$TF) between near-glacier and fjord-mouth CTD profiles across three depth ranges: shallow (0–<50 m), intermediate (50–<250 m), and deep ($\geq$250 m). Results are grouped by region (NW, CW, CE, SE). Each point represents the mean $\delta$TF for one fjord CTD pair within the corresponding depth range. Boxes show the interquartile range (IQR), the horizontal line indicates the median, and whiskers extend to 1.5 $\times$ IQR; statistical outliers are not shown. Filled grey circles indicate fjords with sill depths $\leq$300 m, while open circles indicate sill depths $>$ 300 m. The dashed horizontal line denotes $\delta$TF = 0, where thermal forcing at the glacier equals that at the fjord mouth. Positive values indicate greater thermal forcing near the glacier.

The resulting distributions (Fig. 3; Table 1) show that thermal forcing is lower near glaciers than at the fjord mouth in the upper 50 m across all four regions. NW has the largest median difference ($-2.224$°C), while CW has the smallest ($-1.726$°C). The large interquartile ranges (IQRs) at shallow depths indicate substantial variability between fjords. At intermediate depths, this pattern weakens and partially reverses: CE and CW show higher thermal forcing near glaciers, NW shows little difference, while SE remains lower. Below 250 m, thermal forcing near glaciers converges towards fjord-mouth values across all regions, with smaller IQRs indicating reduced inter-fjord variability. Fjords with sills $\leq$300 m show no clear difference in $\delta TF$ at shallow or intermediate depths, but exhibit more negative $\delta TF$ below 250 m. SE has the most negative $\delta TF$ overall and the greatest inter-fjord variability.

We use the percentage deviation in melt rate (PDS; Equation 3) to quantify how differences in thermal forcing between near-glacier and fjord-mouth locations influence predicted melt rates, while holding all other variables (e.g., water velocity and salinity) constant (Fig. 4e-h). At the surface, cooler waters near glacier termini reduce thermal forcing, corresponding to approximately 50% lower predicted melt rates across all regions. At intermediate depths, however, increased thermal forcing

https://doi.org/10.5194/egusphere-2026-5769
Preprint. Discussion started: 2 October 2026
© Author(s) 2026. CC BY 4.0 License.

**Table 1.** Summary statistics of the difference in thermal forcing between glacier and fjord-mouth surface waters ($\delta TF$) by depth layer and region. IQR = interquartile range; $n$ = number of fjords. Full distributions, including Q1 and Q3, are shown in Fig. 3.

| Depth layer | Region | Median $\delta$TF (°C) | IQR (°C) | $n$ |
|---|---|---|---|---|
| Shallow (0–50 m) | NW | −2.224 | 2.073 | 21 |
| | CW | −1.726 | 2.393 | 9 |
| | CE | −1.740 | 1.562 | 13 |
| | SE | −2.084 | 1.384 | 14 |
| Intermediate (50–250 m) | NW | −0.062 | 0.362 | 21 |
| | CW | 0.210 | 0.218 | 9 |
| | CE | 0.438 | 0.488 | 13 |
| | SE | −0.706 | 0.736 | 14 |
| Deep (>250 m) | NW | −0.149 | 0.319 | 8 |
| | CW | −0.215 | 0.242 | 9 |
| | CE | 0.072 | 0.223 | 7 |
| | SE | −0.498 | 0.569 | 12 |

enhances predicted melt rates by up to 13% in Northwest Greenland, 30% in Central West Greenland, and 132% in Central East Greenland (Fig. 4).

Despite these large percentage increases, the corresponding absolute changes in thermal forcing shown in Figures 4a-c are small, and therefore large PDS values in Fig. 4e-g do not necessarily imply large absolute changes in melt rate. This is particularly important in CE Greenland, where thermal forcing at the fjord mouth approaches zero (Fig. 4c). Because PDS is calculated relative to the melt rate predicted using thermal forcing at the fjord mouth, even a small absolute increase in thermal forcing from a near-zero baseline can produce a large percentage increase in PDS while the resulting melt rates remain relatively small.

### 3.3 Physical drivers of temperature changes

Previous sections show a broadly consistent modification of water properties by fjord processes in all regions except SE Greenland. Here we present two case studies to examine the mechanisms responsible for these changes. Our first case study is Ikerasaap Sullua fjord (Fig. 5), where surface cooling and intermediate warming near the glacier resemble the regional mean pattern observed in NW, CW, and CE Greenland (Fig. 2, Fig. A3a). This fjord drains Sermeq Kujalleq (Store Gletsjer), a marine-terminating glacier with a deep grounding line (480 m) and no shallow sills (defined as a sill $\leq$ 300 m).

The CTD data from Ikerasaap Sullua fjord shows that water properties become increasingly modified with distance from the mouth towards the glacier, particularly in the upper 200 m of the water column (Fig. 5). At the fjord mouth, there is a three-

https://doi.org/10.5194/egusphere-2026-5769
Preprint. Discussion started: 2 October 2026
© Author(s) 2026. CC BY 4.0 License.

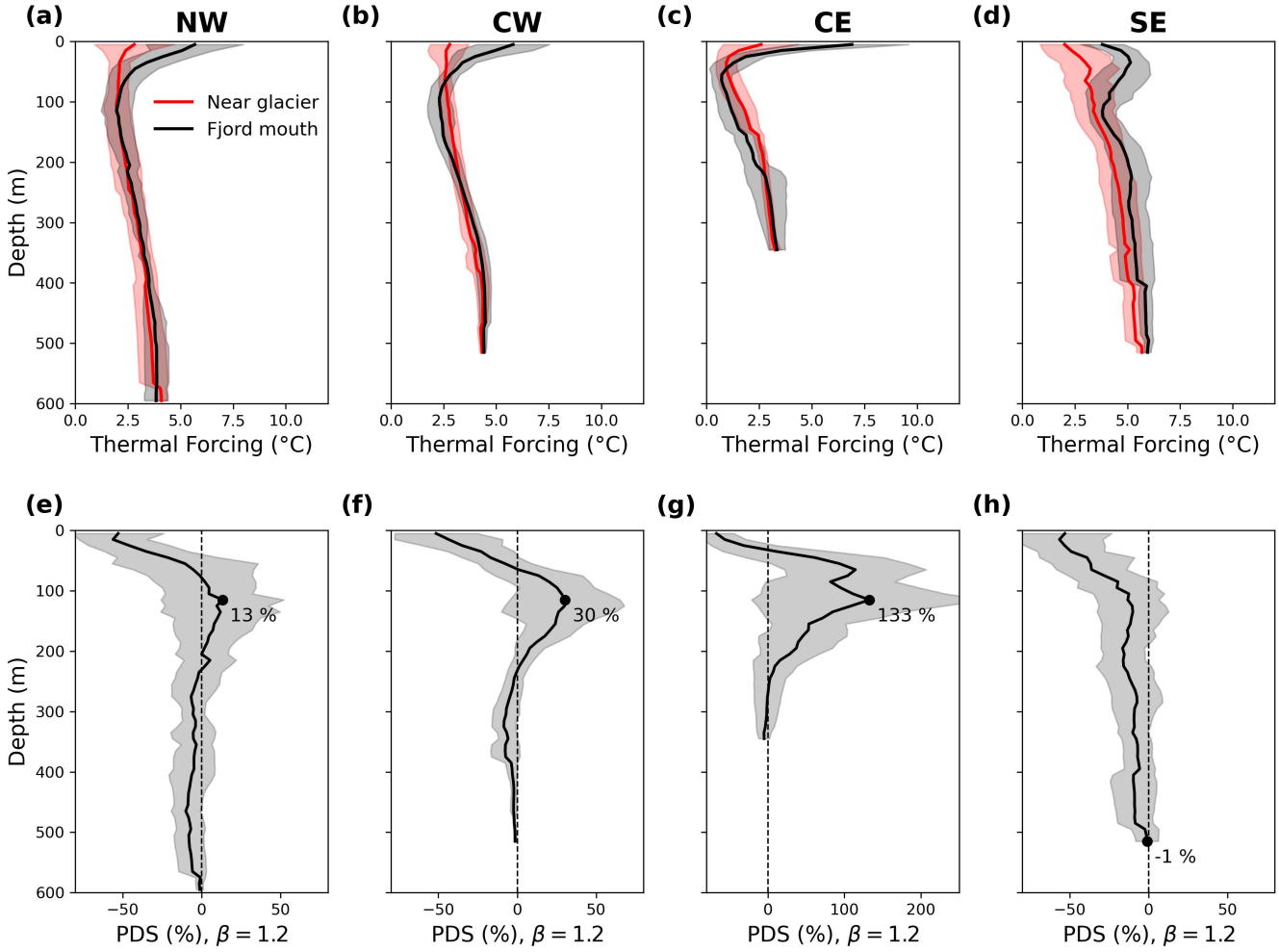


**Figure 4.** (a–d) Regional mean depth profiles of thermal forcing for near-glacier (red) and fjord-mouth (black) CTD profiles in the Northwest (NW), Central West (CW), Central east (CE), and Southeast (SE) regions. (e–h) Percentage difference in submarine melt rate (PDS), calculated from differences in $TF^{1.2}$ between near-glacier and fjord-mouth profiles at each depth (see Methods). For all plots shading indicates $\pm 1$ standard deviation. The black dashed line marks zero difference. Black markers show the depth of maximum PDS. Note the extended x-axis for CE.

layer water mass structure: summer-warmed Polar Water (PWw) overlying cooler PW, with a deep temperature maximum at 400 m corresponding to modified deep Sup-Polar Mode Water (dSPMW), Atlantic Water that has been transported from the Irminger Sea via Cape Farewell and carried north by the West Greenland Current (Rysgaard et al., 2020). Near the glacier, the surface layer is colder and fresher than at the mouth (Fig. 5a), consistent with iceberg melting or runoff input. Between 50 and 200 m the near-glacier profile is warmer than at the fjord mouth and follows parallel to the freshwater mixing line, which is consistent with the intermediate warming being the result of plume-driven upwelling of deep warm dSPMW at the

https://doi.org/10.5194/egusphere-2026-5769
Preprint. Discussion started: 2 October 2026
© Author(s) 2026. CC BY 4.0 License.

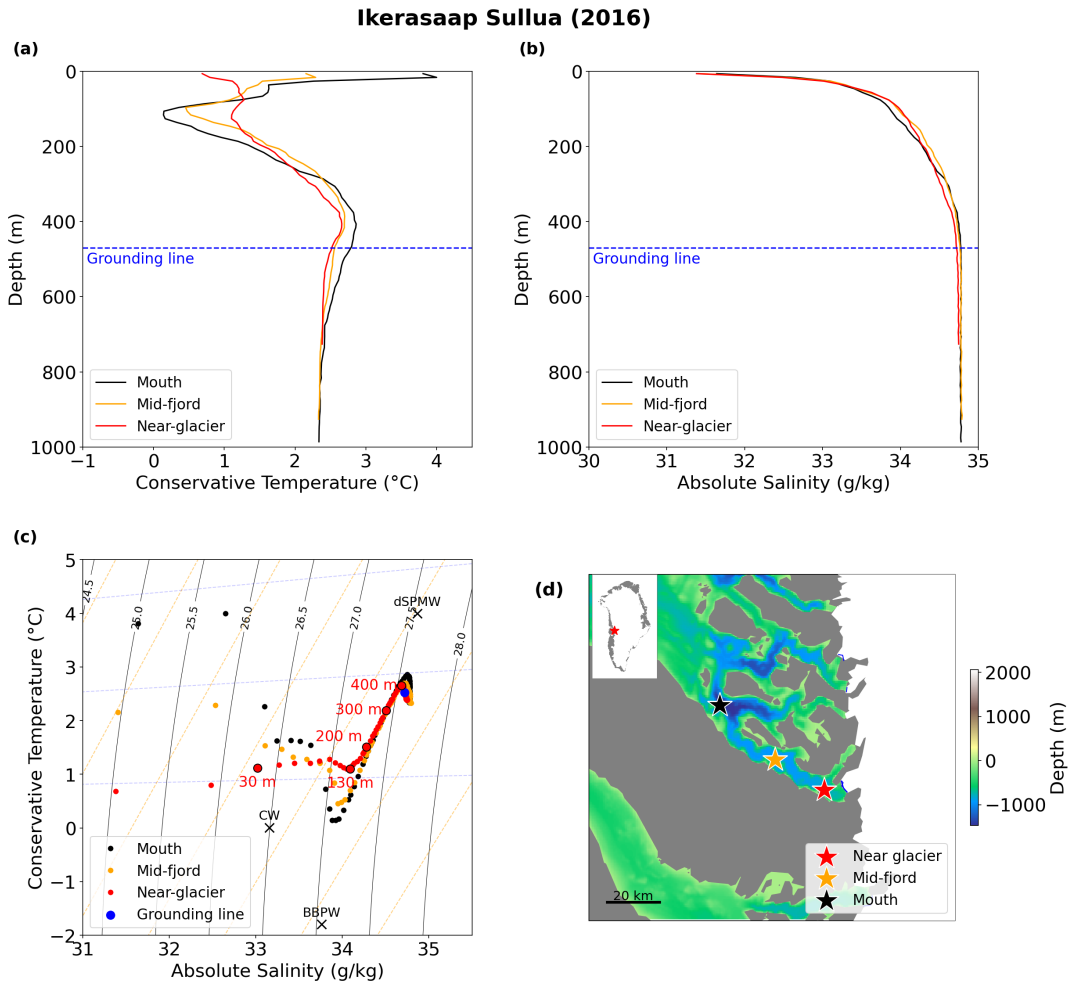


**Figure 5.** CTD profiles from Ikerasaap Sullua fjord (Central West Greenland). Panels show (a) conservative temperature, (b) absolute salinity, and (c) temperature–salinity ($\Theta$–$S$) properties, and (d) a map of CTD locations along the length of the fjord. The colour of each profile denotes profile location. In $\Theta$–$S$ space, dashed orange and blue lines indicate meltwater and freshwater mixing lines, respectively. Circles mark depth levels, including sill depth (grey) and grounding line depth (blue). Black curves are isopycnals. The upper 10 m are omitted due to focus on the changes at depth. Black crosses represent typical temperature and salinity characteristics of different water masses found on the West Greenland shelf and are taken from Rysgaard et al. (2020): dSPMW is deep Sub-Polar Mode Water (a sub-category of Atlantic Water); CW is South West Greenland Coastal Water (a sub-category of Polar Water), and BBPW is Baffin Bay Polar Water.

calving front. Deep water below 250 m in the fjord shows less modification, but the deep AW in the fjord cools glacier-ward, consistent with observations from Kangerlussuaq Fjord (Kangersertuaq in Greenlandic) by (Inall et al., 2014), who attributed the cooling to AW mixing with cooler water masses above and below.

https://doi.org/10.5194/egusphere-2026-5769
Preprint. Discussion started: 2 October 2026
© Author(s) 2026. CC BY 4.0 License.

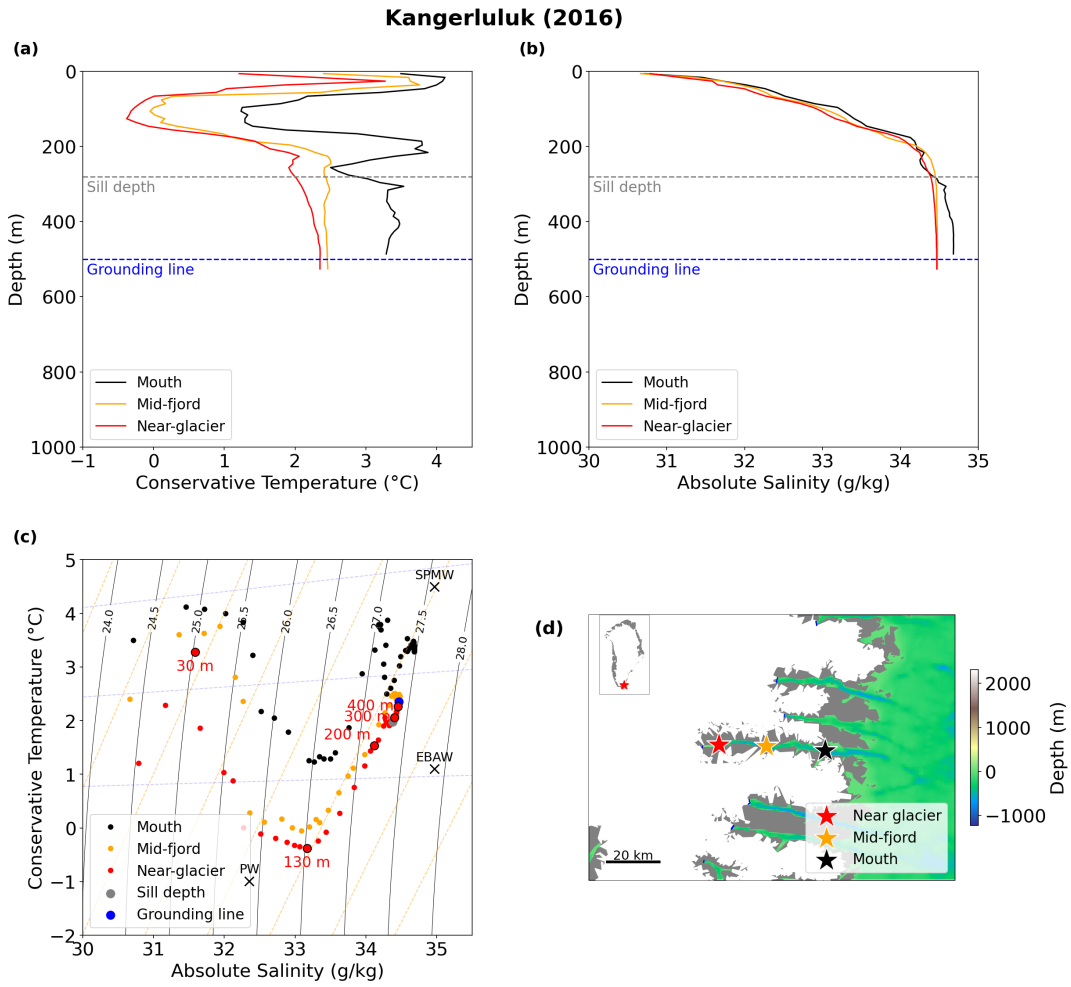


**Figure 6.** CTD profiles from Kangerluluk fjord (South East Greenland). Panels show (a) conservative temperature, (b) absolute salinity, and (c) temperature–salinity ($\Theta$–$S$) properties, and (d) a map of the fjord with bathymetry and CTD locations. Colours denote profile location. In $\Theta$–$S$ space, dashed orange and blue lines indicate meltwater and freshwater mixing lines, respectively. Circles mark depth levels, including sill depth (grey) and grounding line depth (blue). Black curves are isopycnals. The upper 10 m are omitted due to focus on the changes at depth. Black crosses represent typical temperature and salinity characteristics of different water masses found in East Greenland and are taken from Rysgaard et al. (2024): SPMW is Sub-Polar Mode Water (a sub-category of Atlantic Water); EBAW is Eurasian Basin Atlantic Water, and PW is Polar Water.

Fjords in SE Greenland differ from other regions, with near-glacier waters cooler and fresher than fjord-mouth waters and high inter-fjord variability (Fig. 3). Fig. 6 shows CTD profiles from Kangerluluk Fjord, where the near-glacier profile is cooler and fresher than the fjord-mouth profile at all depths (Fig. A3b). Below 300 m, a shallow sill between the fjord mouth and mid-fjord restricts the inflow of warm deep SPMW (Fig. 6a), as indicated by the similarity between deep mid-fjord waters and

https://doi.org/10.5194/egusphere-2026-5769
Preprint. Discussion started: 2 October 2026
© Author(s) 2026. CC BY 4.0 License.

sill-depth properties at the fjord mouth. Above 300 m the cause of the apparent cooling is less clear. The Θ-S diagram (Fig. 6c) shows that mid-fjord and near-glacier profiles follow the Gade line between 130–400 m, indicating a possible role for ice melt, but the significance of this is unclear given the tendency of shelf water properties to plot along this gradient (Straneo et al., 2012). A limitation of this dataset is that most observations in SE Greenland (13/17) were collected within a single field campaign (18 September–4 October 2016), making it hard to assess whether these results are typical of conditions in SE Greenland or represent a combination of shelf and fjord conditions particular to that point in time. This is discussed further in Section 4.

## 4 Discussion

Our results highlight that across Greenland, the transition from the fjord mouth to the glacier is characterised by a substantial and systematic modification of water properties, with near-glacier waters are typically cooler at the surface, warmer at intermediate depths, and only weakly modified below ∼250 m. Although the magnitude of these changes varies substantially between fjords, the consistency of their vertical structure across regions (with the exception of SE Greenland, discussed below) suggests that common near-glacier processes shape fjord hydrography in late summer.

Surface waters near glaciers are almost ubiquitously colder than those at fjord mouths (Fig. 2). This pattern is likely driven by enhanced melting of mélange and icebergs within the warm Polar Surface Water (PSWw) layer (Inall et al., 2014; Davison et al., 2022). In contrast to surface cooling, we find widespread warming at intermediate depths (50–250 m) near glacier termini across Greenland (Figures 2a–d, 4e–h), likely a result of plume-driven upwelling of Atlantic Water (Holland et al., 2008; Straneo et al., 2011; Slater et al., 2018; Mortensen et al., 2020). This pattern extends previous observations from NW Greenland (Cowton et al., 2023) by demonstrating that this subsurface warming is a common feature at glacier termini in late summer, as is cooler surface waters in the top 50 m. Below 250m, we see relatively little modification of fjord waters relative to the shelf, except where shallow sills block the ingress of warm AW at depth.

These observations have important implications for the submarine melting and calving at Greenland's marine terminating glaciers. At the shallowest depths, surface waters at the fjord mouths are often warmed to temperatures in excess of $\sim 5°C$ by late summer, typically making them the warmest waters in the fjords. Melting at the waterline by surface warmed waters can be an important driver of calving (Pętlicki et al., 2015), but our results show that the high iceberg concentrations in Greenland's fjords cool surface waters sufficiently to reduce melting by on average ∼50 % relative to in their absence (Fig. 4e-h), helping to shield the glaciers from this effect. However, there is high variability in the magnitude of surface cooling near glaciers (Figures 2 and3), which could arise from differences in iceberg abundance (Kinne et al., 2025; Davison et al., 2022), freshwater inputs from runoff and subglacial discharge (Mortensen et al., 2020), and air-sea heat exchange (Christoffersen et al., 2011). At intermediate depths however, where very cold Polar Waters inhibit melting, the upwelling of warm Atlantic Water by subglacial discharge plumes provide a key source of heat. Although the increase in thermal forcing from these plumes is modest (<1°C), the relative impact of this warming in this cold layer is significant, in some instances leading to a two-fold increase in submarine melt rates relative to the unmodified Polar Water (Fig. 4). The combined effect of this modification is to

https://doi.org/10.5194/egusphere-2026-5769
Preprint. Discussion started: 2 October 2026
© Author(s) 2026. CC BY 4.0 License.

reduce vertical variation in the melt rate. Given that calving is sensitive to both the rate and vertical distribution of submarine melting (Slater et al., 2021), these effects may be important in influencing the way in which changes in shelf water properties translate into impacts on submarine melting and calving.

An important motivation in this work is the desire to improve the ocean forcing applied in ice sheet modelling studies. Because there are few observations in fjords, and fjords are not well resolved in ocean models, ice sheet models are typically forced using a frontal ablation parameterisation based on water properties on the shelf. As our results show, these may differ substantially from the properties of the fjord waters adjacent to glacier termini, potentially introducing error into this forcing. How significant this error is likely to be depends on the forcing used. For simplicity, it is common to focus on deep water temperatures (>200 m) in ocean forcing parameterisations (e.g. (Slater et al., 2020; Rignot et al., 2016)). Our results demonstrate that at this depth, fjord waters are relatively unmodified by ice melt and plume-driven upwelling, and so along-fjord temperature differences are typically small (Fig. 2). Accordingly, such parameterisations are likely relatively insensitive to in-fjord processes, except where shallow sills are present, which is relatively easy to account for Slater et al. (2020). This does not however mean that the modification at shallower depths is not important for marine terminating glaciers or the modelling of these glaciers. As models become more sophisticated, more complex melting and calving approaches, capable of better incorporating vertical variability at the calving front are likely to become increasingly important (Wheel et al., 2024; Cook et al., 2022; van Dongen et al., 2020; Benn et al., 2017). As such, the need to account for fjord modification of water properties is only likely to grow, and our results support the development of coupled fjord–ice-sheet modelling frameworks that explicitly account for near-glacier water modification where observations are unavailable.

There are some limitations to what can be shown by this study. In particular, SE Greenland stands out as an exception to the trends observed in the other regions, with water in fjords anomalously cooler and fresher than those at fjord mouths throughout the water column (Fig. 2). The conditions do not align with the expected impacts of iceberg melt and plume-driven upwelling as seen across the other regions, and it is unclear why the physical processes, or their impacts, should be distinct in these fjords from elsewhere in Greenland. Instead, we suggest the anomalous results may be linked to the regional setting and the timing of observations. SE Greenland experiences highly variable shelf conditions on synoptic and seasonal timescales (Harden et al., 2014). Mooring data from the shelf near Sermilik fjord (Harden et al., 2014) and temperature data from tagged seals across SE Greenland (Sutherland et al., 2013) observed warm water intrusions at shallow depths in autumn on the SE Greenland continental shelf. Most of the CTD observations from this region come from a 2 week window in Sept/Oct 2016, so it is possible that the apparent offset between fjord and shelf conditions could result from a recent change in shelf conditions that had not yet propagated into the fjords; in this scenario, observations obtained on a different date or year may give quite different results. This explanation does however remain speculative until it can be tested against further observations. More generally, it should be emphasized that observations in all regions come from late summer and early autumn, and the magnitude of the observed effects is likely to vary significantly from season to season, with subglacial discharge and near-surface iceberg melt both likely greatly decreased during winter.

https://doi.org/10.5194/egusphere-2026-5769
Preprint. Discussion started: 2 October 2026
© Author(s) 2026. CC BY 4.0 License.

## 5 Conclusions

We have analysed water properties adjacent to 38 Greenland fjords between 2016 and 2021. We find a consistent depth-dependent pattern of fjord modification: surface waters are cooled, intermediate waters are warmed, and deep waters are comparatively unchanged relative to fjord-mouth conditions. This vertical structure is widespread across Greenland, with the exception of SE Greenland, where the cause of the difference in fjord and shelf water temperature and salinity remains unclear.

These results demonstrate that far-field thermal forcing on the shelf is not analogous to thermal forcing near glaciers. Fjord modification is most pronounced in the upper 250 m of the water column. This suggests that glacier retreat implementations that account for fjord bathymetry and use thermal forcing at grounding line depth or at depths below 250 m (eg Slater et al. (2020)) may be more robust against fjord modification. However, more sophisticated models that include vertically-varying undercut/overcut ice geometries will need better thermal forcing data throughout the water column.

We suggest that future progress in predicting ocean-driven glacier change requires improved representation of near-glacier fjord processes. In the absence of direct observations, this may be achieved through coupled fjord–ice-sheet–ocean modelling frameworks that resolve the vertical structure of fjord modification and its influence on submarine melt forcing.

*Code and data availability.* The data used in the creation of the manuscript can be accessed at Cameron et al. (2026a), with a CC-BY license. The CTD and AXCTD data were obtained from the Oceans Melting Greenland project, and are available from OMG (2020). and OMG (2019) respectively. Sill depths and grounding line depths can be accessed from Mas e Braga (2025), and additional fjord bathymetry can be accessed from Morlighem et al. (2022). The code used for processing and plotting all figures in the manuscript can be accessed at Cameron et al. (2026b) under the MIT license, with instructions and dependencies listed in the README.md file.

## Appendix A: Additional supporting results

### A1 Thermal forcing and PDS Results, $\beta = 1.6$

Results in the manuscript assume that melt rate scales with $TF^{1.2}$. Xu et al. (2013) showed that melt rate can scale with $TF^{1.2}$ when rates of subglacial discharge are high, and with $TF^{1.6}$ when subglacial discharge is lower. Here we present the same results as Fig. 3 in the paper, but the scaling factor $\beta$ is set as 1.6 to give a broader range of possible results. Note that increasing the scaling factor increases the percentage difference in submarine melt rate (PDS) between the mouth and near-fjord profiles.

https://doi.org/10.5194/egusphere-2026-5769
Preprint. Discussion started: 2 October 2026
© Author(s) 2026. CC BY 4.0 License.

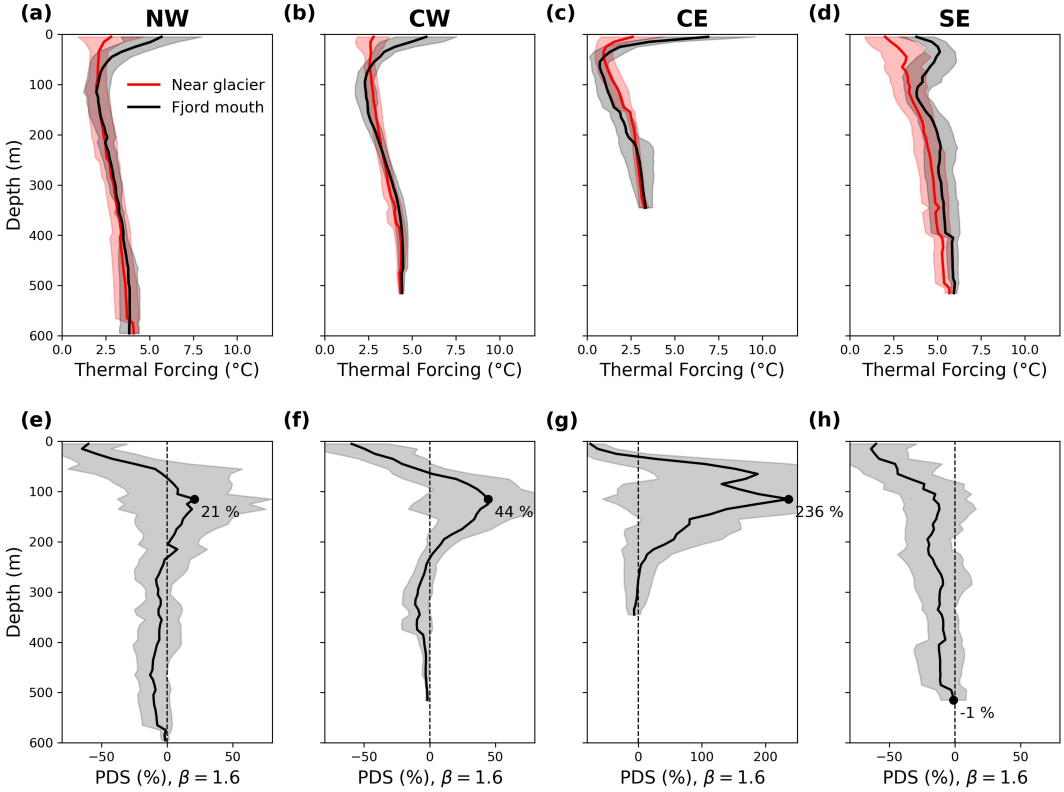


**Figure A1.** (a–d) Regional mean depth profiles of thermal forcing for near-glacier (red) and fjord-mouth (black) CTD profiles in the Northwest (NW), Central West (CW), Central east (CE), and Southeast (SE) regions. (e–h) Percentage difference in submarine melt rate (PDS), calculated from differences in $TF^{1.6}$ between near-glacier and fjord-mouth profiles at each depth. For all plots shading indicates $\pm 1$ standard deviation. The black dashed line marks zero difference. Black markers show the depth of maximum PDS. Note the extended x-axis for CE.

https://doi.org/10.5194/egusphere-2026-5769
Preprint. Discussion started: 2 October 2026
© Author(s) 2026. CC BY 4.0 License.

## A2 Temperature-Salinity properties of Kangersertuaq Fjord, CE Greenland.

Kangersertuaq Fjord (also known as Kangerlussuaq Fjord in East Greenland) stands out in Fig. 2 due to its prominent cold anomaly from 250-400 m depth. The dense mélange in Kangersertuaq fjord means that the near-glacier CTD is 21 km from the ice-front, so will be modified relative to the water in contact with the ice front. The raw profiles and temperature-salinity diagram in Fig. S2 suggest that this deep cold anomaly is caused by the absence of warm AWm near the glacier.

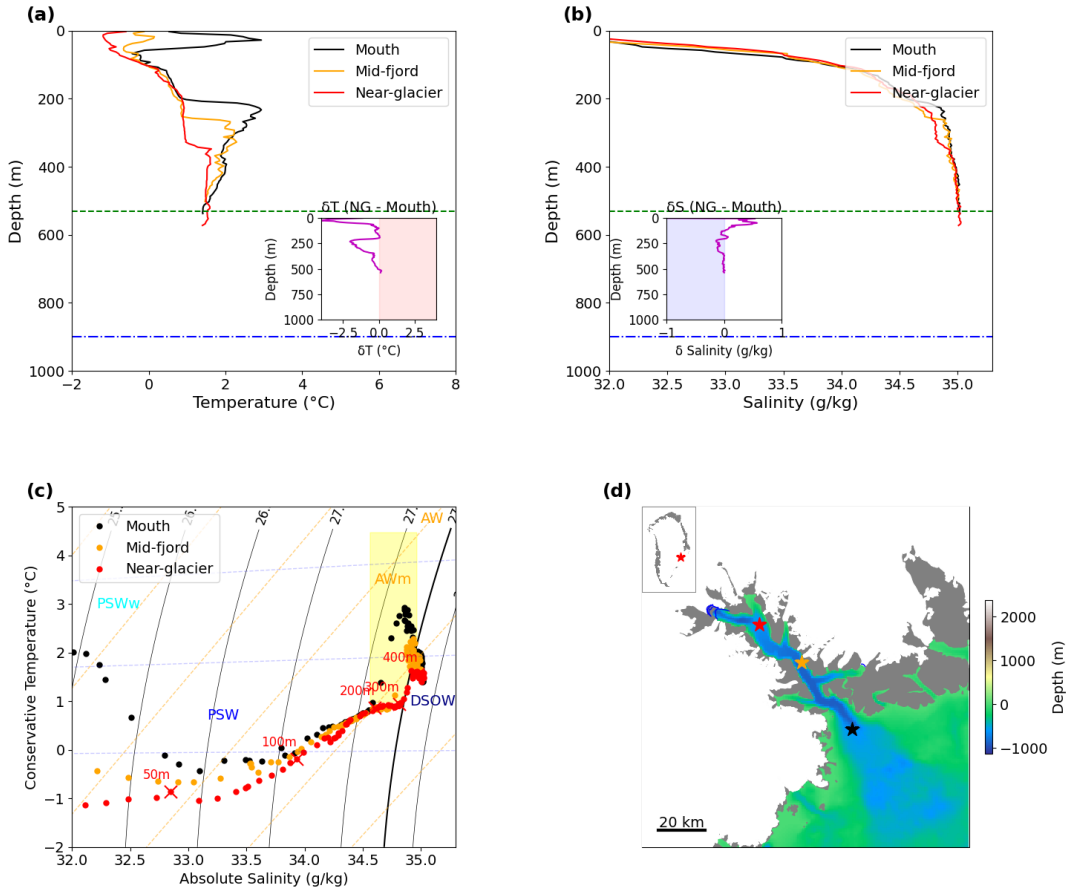


**Figure A2.** Depth profiles of (a) conservative temperature and (b) absolute salinity for Kangersertuaq fjord in Central East Greenland. CTDs include a profile in the near-glacier region (red), mid-fjord (orange) and at the fjord mouth (black). Profiles are binned into 10 m bins. The inset in (a) shows the temperature difference between the mouth and near-glacier profiles. The inset in (b) shows the salinity difference between the near-glacier and mouth profiles. (c) Profiles corresponding to those in (a) and (b) shown in conservative temperature-absolute salinity (TS) space. Gade lines and freshwater mixing lines are indicated by orange and blue dashed lines respectively. Crosses indicate depth levels. The shaded region indicates the AWm water mass, defined in Inall et al. (2014). The black curved lines are lines of equal density (isopycnals). The 27.8 isopycnal represents the density boundary separating modified Atlantic Water and Denmark Strait Overflow Water. Note that the axes limits exclude the surface 10 meters.

https://doi.org/10.5194/egusphere-2026-5769
Preprint. Discussion started: 2 October 2026
© Author(s) 2026. CC BY 4.0 License.

## A3 Depth profiles showing the difference in temperature ($\delta$T) between near-glacier and fjord mouth CTDs for Ikerasaap Sullua and Kangerluluk Fjords

In the main text, Fig. 2 shows temperature difference ($\delta$) plots from each region to show the difference in temperature near glaciers relative to the fjord mouth. At regional scales, fjords behave similarly, which could allow the development of a transfer function. These $\delta$T plots accompany Figures 5 and 6 in the main text, to show that Ikerasaap Sullua is broadly representative of the overall trend in fjord modification seen across regions. Kangerluluk is a case study from Southeast Greenland, where fjords appear cooler and fresher at all depths near glaciers relative to fjord mouths.

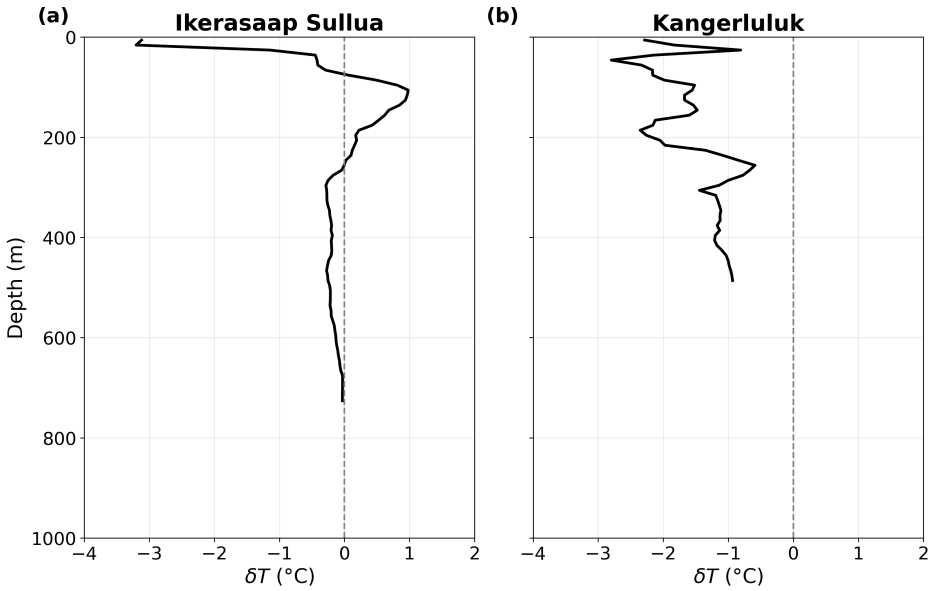


**Figure A3.** Temperature difference ($\delta$T) vs depth plots for (a) Ikerasaap Sullua and (b) Kangerluluk fjords from CTDs taken in 2016 by the OMG project (OMG, 2020).

https://doi.org/10.5194/egusphere-2026-5769
Preprint. Discussion started: 2 October 2026
© Author(s) 2026. CC BY 4.0 License.

*Author contributions.* EC and TC conceptualised the project. EFC performed the analyses under the supervision of TC, AB, and PH. EC wrote the initial manuscript draft. TC, AB, and PH reviewed and edited the manuscript.

*Competing interests.* The authors declare that they have no conflict of interest.

*Acknowledgements.* This work was supported by the NERC IAPETUS2 DTP through grant number NE/S007431/1, and through NE/W00531X/1. This work was supported by the Advanced Research and Invention Agency (ARIA) under the Forecasting Tipping Points programme (Project: GIANT - Greenland Ice sheet to Atlantic tipping points from ice loss). Thank you to TJ Young for his support, and to Donald Slater, Martim Mas e Braga, Neil Fraser and Mark Inall for their thoughtful discussions.

https://doi.org/10.5194/egusphere-2026-5769
Preprint. Discussion started: 2 October 2026
© Author(s) 2026. CC BY 4.0 License.

## References

Bao, W. and Moffat, C.: Impact of shallow sills on circulation regimes and submarine melting in glacial fjords, The Cryosphere, 18, 187–203, https://doi.org/10.5194/tc-18-187-2024, 2024.

Benn, D. I., Åström, J., Zwinger, T., Todd, J., Nick, F. M., Cook, S., Hulton, N. R. J., and Luckman, A.: Melt-under-cutting and buoyancy-driven calving from tidewater glaciers: new insights from discrete element and continuum model simulations, Journal of Glaciology, 63, 691–702, https://doi.org/10.1017/jog.2017.41, 2017.

Bevan, S. L., Luckman, A. J., Benn, D. I., Cowton, T., and Todd, J.: Warming of SE Greenland Shelf Waters in 2016 Primes Large Glacier for Runaway Retreat, The Cryosphere Discuss., https://doi. org/10.5194/tc-2018-260, in review, 2019.

Cameron, E. F., Cowton, T. R., Bradley, A. T., and Holland, P. R.: Paired Fjord-Mouth and Near-Glacier CTD/AXCTD Profiles for 39 Greenlandic Fjords from 2016-2021, https://doi.org/10.17630/8dc6f997-8aa9-43f5-8339-83a0cef63b5b, [Dataset]., 2026a.

Cameron, E. F., Cowton, T. R., Bradley, A. T., and Holland, P. R.: CTD Analysis and Figure Scripts for "Greenland Fjord Processes Have a Depth-Dependent Influence on Predicted Submarine Melt Rates (v2.0), https://doi.org/10.5281/zenodo.22769296, 2026b.

Christoffersen, P., Mugford, R., Heywood, K., Joughin, I., Dowdeswell, J., Syvitski, J., Luckman, A., and Benham, T.: Warming of waters in an East Greenland fjord prior to glacier retreat: mechanisms and connection to large-scale atmospheric conditions, The Cryosphere, 5, 701–714, 2011.

Cook, S. J., Christoffersen, P., and Todd, J.: A fully-coupled 3D model of a large Greenlandic outlet glacier with evolving subglacial hydrology, frontal plume melting and calving, Journal of Glaciology, 68, 486–502, https://doi.org/10.1017/jog.2021.109, 2022.

Cowton, T. R., Slater, D. A., and Inall, M. E.: Subglacial-discharge Plumes Drive Widespread Subsurface Warming in Northwest Greenland's Fjords, Geophysical Research Letters, 50, https://doi.org/10.1029/2023gl103801, 2023.

Davison, B. J., Cowton, T. R., Cottier, F. R., and Sole, A. J.: Iceberg Melting Substantially Modifies Oceanic Heat Flux Towards a Major Greenlandic Tidewater Glacier, Nature Communications, 11, https://doi.org/10.1038/s41467-020-19805-7, 2020.

Davison, B. J., Cowton, T., Sole, A., Cottier, F., and Nienow, P.: Modelling the effect of submarine iceberg melting on glacier-adjacent water properties, The Cryosphere, 16, 1181–1196, https://doi.org/10.5194/tc-16-1181-2022, 2022.

Fenty, I., Willis, J., Khazendar, A., Dinardo, S., Forsberg, R., Fukumori, I., Holland, D., Jakobsson, M., Moller, D., Morison, J., Meunchow, A., Rignot, E., Schodlock, M., Thompson, A., Tino, K., Rutherford, M., and Trenholm, N.: Oceans Melting Greenland: Early results from NASA's ocean-ice mission in Greenland, Oceanography, 29, 72–83, https://doi.org/10.5670/ocean.2016.100, 2016.

Fraser, N. J., Inall, M. E., Magaldi, M. G., Haine, T. W., and Jones, S. C.: Wintertime fjord-shelf interaction and ice sheet melting in southeast Greenland, Journal of Geophysical Research: Oceans, 123, 9156–9177, 2018.

Geyer, W. R. and Cannon, G. A.: Sill processes related to deep water renewal in a fjord, Journal of Geophysical Research: Oceans, 87, 7985–7996, https://doi.org/https://doi.org/10.1029/JC087iC10p07985, 1982.

Gladish, C. V., Holland, D. M., Rosing-Asvid, A., Behrens, J. W., and Boje, J.: Oceanic Boundary Conditions for Jakobshavn Glacier. Part I: Variability and Renewal of Ilulissat Icefjord Waters, 2001–14, Journal of Physical Oceanography, 45, 3 – 32, https://doi.org/10.1175/JPO-D-14-0044.1, 2015.

Goelzer, H., Nowicki, S., Payne, A., Larour, E., Seroussi, H., Lipscomb, W. H., Gregory, J., Abe-Ouchi, A., Shepherd, A., Simon, E., Agosta, C., Alexander, P., Aschwanden, A., Barthel, A., Calov, R., Chambers, C., Choi, Y., Cuzzone, J., Dumas, C., Edwards, T., Felikson, D., Fettweis, X., Golledge, N. R., Greve, R., Humbert, A., Huybrechts, P., Le clec'h, S., Lee, V., Leguy, G., Little, C., Lowry, D. P., Morlighem, M., Nias, I., Quiquet, A., Rückamp, M., Schlegel, N. J., Slater, D. A., Smith, R. S., Straneo, F., Tarasov, L., van de Wal, R., and van den

https://doi.org/10.5194/egusphere-2026-5769
Preprint. Discussion started: 2 October 2026
© Author(s) 2026. CC BY 4.0 License.

Broeke, M.: The future sea-level contribution of the Greenland ice sheet: a multi-model ensemble study of ISMIP6, The Cryosphere, 14, 3071–3096, https://doi.org/10.5194/tc-14-3071-2020, tC, 2020.

Goliber, S., Black, T., Catania, G., Lea, J. M., Olsen, H., Cheng, D., Bevan, S., Bjørk, A., Bunce, C., Brough, S., et al.: TermPicks: A century of Greenland glacier terminus data for use in machine learning applications, The Cryosphere Discussions, 2021, 1–41, 2021.

Hager, A. O., Sutherland, D. A., Amundson, J. M., Jackson, R. H., Kienholz, C., Motyka, R. J., and Nash, J. D.: Subglacial Discharge Reflux and Buoyancy Forcing Drive Seasonality in a Silled Glacial Fjord, Journal of Geophysical Research: Oceans, 127, e2021JC018 355, https://doi.org/https://doi.org/10.1029/2021JC018355, e2021JC018355 2021JC018355, 2022.

Harden, B. E., Straneo, F., and Sutherland, D. A.: Moored observations of synoptic and seasonal variability in the East Greenland Coastal Current, Journal of Geophysical Research: Oceans, 119, 8838–8857, https://doi.org/https://doi.org/10.1002/2014JC010134, 2014.

Holland, D. M., Thomas, R. H., de Young, B., Ribergaard, M. H., and Lyberth, B.: Acceleration of Jakobshavn Isbræ triggered by warm subsurface ocean waters, Nature Geoscience, 1, 659–664, https://doi.org/10.1038/ngeo316, 2008.

Howat, I. M., Joughin, I., Fahnestock, M., Smith, B. E., and Scambos, T. A.: Synchronous retreat and acceleration of southeast Greenland outlet glaciers 2000–06: ice dynamics and coupling to climate, Journal of Glaciology, 54, 646–660, https://doi.org/10.3189/002214308786570908, 2008.

Inall, M. E., Murray, T., Cottier, F. R., Scharrer, K., Boyd, T. J., Heywood, K. J., and Bevan, S. L.: Oceanic Heat Delivery via Kangerdlugssuaq Fjord to the South-east Greenland Ice Sheet, Journal of Geophysical Research: Oceans, 119, 631–645, 2014.

Jackson, R. H., Straneo, F., and Sutherland, D. A.: Externally Forced Fluctuations in Ocean Temperature at Greenland Glaciers in Non-summer Months, Nature Geoscience, 7, 503–508, https://doi.org/10.1038/ngeo2186, 2014.

Jenkins, A.: Convection-driven melting near the grounding lines of ice shelves and tidewater glaciers, Journal of Physical Oceanography, 41, 2279–2294, 2011.

King, M. D., Howat, I. M., Jeong, S., Noh, M. J., Wouters, B., Noël, B., and van den Broeke, M. R.: Seasonal to decadal variability in ice discharge from the Greenland Ice Sheet, The cryosphere, 12, 3813–3825, 2018.

Kinne, K., Sanchez, R., Siegelman, L., Straneo, F., and Hughes, K.: The seasonality of Greenland iceberg melt and its influences on fjord properties and dynamics, Journal of Geophysical Research: Oceans, 130, e2025JC022 587, 2025.

Lea, J. M.: The Google Earth Engine Digitisation Tool (GEEDiT) and the Margin Change Quantification Tool (MaQiT) – Simple Tools for the Rapid Mapping and Quantification of Changing Earth Surface Margins, Earth Surface Dynamics, 6, 551–561, https://doi.org/10.5194/esurf-6-551-2018, 2018.

Mankoff, K. D., Fettweis, X., Langen, P. L., Stendel, M., Kjeldsen, K. K., Karlsson, N. B., Noël, B., van den Broeke, M. R., Solgaard, A., Colgan, W., Box, J. E., Simonsen, S. B., King, M. D., Ahlstrøm, A. P., Andersen, S. B., and Fausto, R. S.: Greenland ice sheet mass balance from 1840 through next week, Earth System Science Data, 13, 5001–5025, https://doi.org/10.5194/essd-13-5001-2021, 2021.

Mas e Braga, M.: Supplementary datasets for Mas e Braga et al., "Controls on fjord temperature throughout Greenland in a reduced-physics model" , https://doi.org/10.5281/zenodo.15880691, 2025.

McDougall, T. J. and Barker, P. M.: Getting Started with TEOS-10 and the Gibbs Seawater (GSW) Oceanographic Toolbox, Scor/iapso WG, 127, 1–28, 2011.

Meier, W. N. and Stroeve, J.: An updated assessment of the changing Arctic sea ice cover, Oceanography, 35, 10–19, 2022.

Morlighem, M., Rignot, E., Mouginot, J., Seroussi, H., and Larour, E.: IceBridge BedMachine Greenland, Version 5, https://doi.org/10.5067/GMEVBWFLWA7X, 2022.

https://doi.org/10.5194/egusphere-2026-5769
Preprint. Discussion started: 2 October 2026
© Author(s) 2026. CC BY 4.0 License.

Mortensen, J., Lennert, K., Bendtsen, J., and Rysgaard, S.: Heat sources for glacial melt in a sub-Arctic fjord (Godthåbsfjord) in contact with the Greenland Ice Sheet, Journal of Geophysical Research: Oceans, 116, https://doi.org/https://doi.org/10.1029/2010JC006528, 2011.

Mortensen, J., Rysgaard, S., Bendtsen, J., Lennert, K., Kanzow, T., Lund, H., and Meire, L.: Subglacial discharge and its down-fjord transformation in West Greenland fjords with an ice mélange, Journal of Geophysical Research: Oceans, 125, e2020JC016 301, 2020.

Mortensen, J., Rysgaard, S., Winding, M. H. S., Juul-Pedersen, T., Arendt, K. E., Lund, H., Stuart-Lee, A. E., and Meire, L.: Multidecadal Water Mass Dynamics on the West Greenland Shelf, Journal of Geophysical Research: Oceans, 127, e2022JC018 724, https://doi.org/https://doi.org/10.1029/2022JC018724, e2022JC018724 2022JC018724, 2022.

Motyka, R. J., Hunter, L., Echelmeyer, K. A., and Connor, C.: Submarine melting at the terminus of a temperate tidewater glacier, LeConte Glacier, Alaska, USA, Annals of Glaciology, 36, 57–65, 2003.

Motyka, R. J., Truffer, M., Fahnestock, M., Mortensen, J., Rysgaard, S., and Howat, I.: Submarine melting of the 1985 Jakobshavn Isbræ floating tongue and the triggering of the current retreat, Journal of Geophysical Research: Earth Surface, 116, https://doi.org/https://doi.org/10.1029/2009JF001632, 2011.

Mouginot, J., Rignot, E., Bjørk, A. A., Van den Broeke, M., Millan, R., Morlighem, M., Noël, B., Scheuchl, B., and Wood, M.: Forty-six Years of Greenland Ice Sheet Mass Balance from 1972 to 2018, Proceedings of the National Academy of Sciences, 116, 9239–9244, 2019.

Nilsson, J., van Dongen, E., Jakobsson, M., O'Regan, M., and Stranne, C.: Hydraulic suppression of basal glacier melt in sill fjords, The Cryosphere, 17, 2455–2476, 2023.

OMG: OMG AXCTD Profiles Ver. 1. PO.DAAC, CA, USA., https://doi.org/10.5067/OMGEV-AXCT1, 2019.

OMG: OMG CTD Conductivity Temperature Depth, https://doi.org/10.5067/OMGEV-CTDS1, 2020.

Otosaka, I. N., Shepherd, A., Ivins, E. R., Schlegel, N.-J., Amory, C., van den Broeke, M. R., Horwath, M., Joughin, I., King, M. D., Krinner, G., Nowicki, S., Payne, A. J., Rignot, E., Scambos, T., Simon, K. M., Smith, B. E., Sørensen, L. S., Velicogna, I., Whitehouse, P. L., A, G., Agosta, C., Ahlstrøm, A. P., Blazquez, A., Colgan, W., Engdahl, M. E., Fettweis, X., Forsberg, R., Gallée, H., Gardner, A., Gilbert, L., Gourmelen, N., Groh, A., Gunter, B. C., Harig, C., Helm, V., Khan, S. A., Kittel, C., Konrad, H., Langen, P. L., Lecavalier, B. S., Liang, C.-C., Loomis, B. D., McMillan, M., Melini, D., Mernild, S. H., Mottram, R., Mouginot, J., Nilsson, J., Noël, B., Pattle, M. E., Peltier, W. R., Pie, N., Roca, M., Sasgen, I., Save, H. V., Seo, K.-W., Scheuchl, B., Schrama, E. J. O., Schröder, L., Simonsen, S. B., Slater, T., Spada, G., Sutterley, T. C., Vishwakarma, B. D., van Wessem, J. M., Wiese, D., van der Wal, W., and Wouters, B.: Mass balance of the Greenland and Antarctic ice sheets from 1992 to 2020, Earth System Science Data, 15, 1597–1616, https://doi.org/10.5194/essd-15-1597-2023, 2023.

Pętlicki, M., Ciepły, M., Jania, J. A., Promińska, A., and Kinnard, C.: Calving of a tidewater glacier driven by melting at the waterline, Journal of Glaciology, 61, 851–863, https://doi.org/10.3189/2015JoG15J062, 2015.

Rignot, E., Xu, Y., Menemenlis, D., Mouginot, J., Scheuchl, B., Li, X., Morlighem, M., Seroussi, H., den Broeke, M. v., Fenty, I., Cai, C., An, L., and Fleurian, B. d.: Modeling of ocean-induced ice melt rates of five west Greenland glaciers over the past two decades, Geophysical Research Letters, 43, 6374–6382, https://doi.org/https://doi.org/10.1002/2016GL068784, 2016.

Rysgaard, S., Boone, W., Carlson, D., Sejr, M., Bendtsen, J., Juul-Pedersen, T., Lund, H., Meire, L., and Mortensen, J.: An updated view on water masses on the pan-west Greenland continental shelf and their link to proglacial fjords, Journal of Geophysical Research: Oceans, 125, e2019JC015 564, 2020.

Rysgaard, S., Mortensen, J., Haxen, M., Gillard, L. C., and Risgaard-Petersen, N.: Summer Hydrography Conditions at Proglacial Fjord Entrances Along East Greenland, Journal of Geophysical Research: Oceans, 129, e2023JC020 665, https://doi.org/https://doi.org/10.1029/2023JC020665, 2024.

https://doi.org/10.5194/egusphere-2026-5769
Preprint. Discussion started: 2 October 2026
© Author(s) 2026. CC BY 4.0 License.

Slater, D. A., Straneo, F., Das, S. B., Richards, C. G., Wagner, T. J. W., and Nienow, P. W.: Localized Plumes Drive Front-Wide Ocean Melting of a Greenlandic Tidewater Glacier, Geophysical Research Letters, 45, 12,350–12,358, https://doi.org/10.1029/2018gl080763, 2018.

Slater, D. A., Felikson, D., Straneo, F., Goelzer, H., Little, C. M., Morlighem, M., Fettweis, X., and Nowicki, S.: Twenty-first Century Ocean Forcing of the Greenland Ice Sheet for Modelling of Sea Level Contribution, The Cryosphere, 14, 985–1008, https://doi.org/10.5194/tc-14-985-2020, 2020.

Slater, D. A., Benn, D. I., Cowton, T. R., Bassis, J. N., and Todd, J. A.: Calving Multiplier Effect Controlled by Melt Undercut Geometry, Journal of Geophysical Research: Earth Surface, 126, e2021JF006 191, 2021.

Smith, R. S., Mathiot, P., Siahaan, A., Lee, V., Cornford, S. L., Gregory, J. M., Payne, A. J., Jenkins, A., Holland, P. R., Ridley, J. K., and Jones, C. G.: Coupling the U.K. Earth System Model to Dynamic Models of the Greenland and Antarctic Ice Sheets, Journal of Advances in Modeling Earth Systems, 13, e2021MS002 520, https://doi.org/https://doi.org/10.1029/2021MS002520, 2021.

Spall, M. A., Jackson, R. H., and Straneo, F.: Katabatic Wind-Driven Exchange in Fjords, Journal of Geophysical Research: Oceans, 122, 8246–8262, https://doi.org/https://doi.org/10.1002/2017JC013026, 2017.

Straneo, F. and Cenedese, C.: The dynamics of Greenland's glacial fjords and their role in climate, Annual review of marine science, 7, 89–112, 2015.

Straneo, F., Curry, R. G., Sutherland, D. A., Hamilton, G. S., Cenedese, C., Våge, K., and Stearns, L. A.: Impact of fjord dynamics and glacial runoff on the circulation near Helheim Glacier, Nature Geoscience, 4, 322–327, https://doi.org/10.1038/ngeo1109, 2011.

Straneo, F., Sutherland, D. A., Holland, D., Gladish, C., Hamilton, G. S., Johnson, H. L., Rignot, E., Xu, Y., and Koppes, M.: Characteristics of Ocean Waters Reaching Greenland's Glaciers, Annals of Glaciology, 53, 202–210, https://doi.org/10.3189/2012aog60a059, 2012.

Sutherland, D. A. and Pickart, R. S.: The East Greenland Coastal Current: Structure, Variability, and Forcing, Progress in Oceanography, 78, 58–77, https://doi.org/https://doi.org/10.1016/j.pocean.2007.09.006, 2008.

Sutherland, D. A., Straneo, F., Stenson, G. B., Davidson, F. J., Hammill, M. O., and Rosing-Asvid, A.: Atlantic water variability on the SE Greenland continental shelf and its relationship to SST and bathymetry, Journal of Geophysical Research: Oceans, 118, 847–855, 2013.

Sutherland, D. A., Roth, G. E., Hamilton, G. S., Mernild, S. H., Stearns, L. A., and Straneo, F.: Quantifying flow regimes in a Greenland glacial fjord using iceberg drifters, Geophysical Research Letters, 41, 8411–8420, https://doi.org/https://doi.org/10.1002/2014GL062256, 2014.

van Dongen, E. C. H., Åström, J. A., Jouvet, G., Todd, J., Benn, D. I., and Funk, M.: Numerical Modeling Shows Increased Fracturing Due to Melt-Undercutting Prior to Major Calving at Bowdoin Glacier, Frontiers in Earth Science, Volume 8 - 2020, https://doi.org/10.3389/feart.2020.00253, 2020.

Watanabe, M., Suzuki, T., O'ishi, R., Komuro, Y., Watanabe, S., Emori, S., Takemura, T., Chikira, M., Ogura, T., Sekiguchi, M., Takata, K., Yamazaki, D., Yokohata, T., Nozawa, T., Hasumi, H., Tatebe, H., and Kimoto, M.: Improved Climate Simulation by MIROC5: Mean States, Variability, and Climate Sensitivity, Journal of Climate, 23, 6312–6335, https://doi.org/https://doi.org/10.1175/2010JCLI3679.1, 2010.

Wheel, I., Benn, D. I., Crawford, A. J., Todd, J., and Zwinger, T.: A new 3D full-Stokes calving algorithm within Elmer/Ice (v9.0), Geoscientific Model Development, 17, 5759–5777, https://doi.org/10.5194/gmd-17-5759-2024, 2024.

Wood, M., Rignot, E., Fenty, I., An, L., Bjørk, A., van den Broeke, M., Cai, C., Kane, E., Menemenlis, D., Millan, R., Morlighem, M., Mouginot, J., Noël, B., Scheuchl, B., Velicogna, I., Willis, J. K., and Zhang, H.: Ocean forcing drives glacier retreat in Greenland, Science Advances, 7, eaba7282, https://doi.org/10.1126/sciadv.aba7282, 2021.

https://doi.org/10.5194/egusphere-2026-5769
Preprint. Discussion started: 2 October 2026
© Author(s) 2026. CC BY 4.0 License.

Xu, Y., Rignot, E., Fenty, I., Menemenlis, D., and Flexas, M. M.: Subaqueous melting of Store Glacier, west Greenland from three-dimensional, high-resolution numerical modeling and ocean observations, Geophysical Research Letters, 40, 4648–4653, https://doi.org/https://doi.org/10.1002/grl.50825, 2013.